LM-04K171
January 26, 2005

Experimental Measurements of Delayed Fission Product Gamma-Ray Transmission Through Low Enriched UO_2 Fuel Pin Lattices in Air

T Trumbull, D Harris

NOTICE

EXPERIMENTAL MEASUREMENTS OF DELAYED FISSION PRODUCT GAMMA-RAY TRANSMISSION THROUGH LOW ENRICHED UO_2 FUEL PIN LATTICES IN AIR

Dr. Timothy H. Trumbull* and Dr. Donald R. Harris

Rensselaer Polytechnic Institute
Department of Mechanical, Aerospace and Nuclear Engineering
110 8th Street
Troy, NY 12180

* To which all correspondence should be directed. Email: trumbt2@rpi.edu.

EXPERIMENTAL MEASUREMENTS OF DELAYED FISSION PRODUCT GAMMA-RAY TRANSMISSION THROUGH LOW ENRICHED UO_2 FUEL PIN LATTICES IN AIR

Dr. Timothy H. Trumbull* and Dr. Donald R. Harris

ABSTRACT

Experimental measurements of delayed fission-product gamma-ray transmission through low-enriched UO_2 fuel pin lattices in an air medium were conducted at the Rensselaer Polytechnic Institute Reactor Critical Facility (RCF). The RCF core consists of excess Special Power Excursion Reactor Test (SPERT) fuel pins, enriched to 4.81 weight percent ^{235}U, clad in stainless steel. An experimental apparatus was constructed to hold various arrangements of fuel pin lattices. The arrangements consisted of a single activated source pin taken from the reactor core surrounded by inactive fuel pins in an air medium. A sodium-iodide detector and gamma-ray spectroscopy system was used to generate a pulse-height spectrum of the gamma-ray radiation for detector positions outside the lattice. The change in radiation intensity as the detector is rotated about the vertical axis of the lattice, the "channeling effect," was measured. Experimental measurements of the channeling effect were performed for six arrangements; 3x3, 5x5, and 7x7 lattices, with both the corner position and center position containing the activated pin. The results of the measurements demonstrate that the gamma-ray radiation intensity can vary widely, as a function of angle, relative to the vertical axis of the lattice.

* To which all correspondence should be directed. Email: trumbt2@rpi.edu.

I. INTRODUCTION

Following reactor shutdown, the gamma-ray radiation from spent nuclear fuel is primarily the result of the decay of longer-lived fission products. Accurately measuring and calculating the gamma-ray radiation from spent fuel is important for exposure control and spent-fuel management, particularly when the fuel has been removed from wet storage.[2] Other applications, such as gamma-scanning of individual fuel pins and gamma-ray tomography of fuel bundles also require accurate measurements of the delayed fission-product gamma-ray radiation.[3,4]

In the case where spent fuel takes the form of fuel rods arranged in lattices, the radiation on the outside of the lattice is not constant. At a fixed distance from the center of the fuel bundle, the radiation intensity changes as a function of angle about the bundle's vertical axis. The effect is due to lower attenuating "paths" through the bundle created by the arrangement of the fuel rods within the lattice. This effect is termed the "channeling effect" and its magnitude is dependent on the characteristics of the lattice, e.g., lattice pitch, number of fuel rods, fuel rod diameter. Therefore, understanding the channeling effect on gamma-ray radiation through fuel pin lattices is an important aspect of performing measurements and analysis of spent nuclear fuel.

In this work, the channeling effect is measured for various arrangements of fuel pins using the RCF. The RCF is a low-power critical facility that allowed for a unique approach to conducting the measurements. The low-power operating characteristics of the RCF (15 W maximum power level, usually not exceeding 3 W indicated power) allow for the rapid transfer of activated fuel pins from the core following shutdown to the measurement apparatus, with minimal personnel exposure concerns.

Along with the approximately 330 fuel pins needed for criticality in the core, the RCF maintains an inventory of unirradiated fuel pins. By surrounding a single activated source pin with unirradiated pins, the channeling effect for specific lattice positions was measured

II. EXPERIMENTAL CONFIGURATION

Measurement Apparatus

An apparatus was constructed consisting primarily of four components: lattice plates, lattice plate support assembly, lattice plate support base, and detector support assembly. The lattice plates were constructed previously for use in the RCF core support structure as part of the conversion from high enriched plate fuel to low enriched SPERT fuel pins. The lattice plates are constructed of stainless steel with the top lattice plate pin holes bored to 1.27 cm (0.5 in) diameter. The bottom lattice plate has holes bored to accommodate a positioning dowel on the lower end cap of the fuel pin. Both plates are drilled with the identical hole pattern with hole centers on a 1.56 cm (0.613 in) square pitch. Sketches of the top and bottom lattice plates are shown in Figure

The lattice plate support assembly is constructed entirely of wood, holds the top and bottom lattice plates in the correct position, and mounts to the lattice plate support

The lattice plate support base is also constructed of wood. The mounting connection allows for the lattice plate support assembly to be rotated about a specific pin position's vertical axis, relative to the detector support assembly, from 0 to 45 degrees. The lattice plate support base is marked off in 5 degree increments for rotating the lattice plate support assembly. It is also marked as necessary to facilitate positioning the detector support assembly as required for the experiment.

The detector support assembly is also constructed of wood and is designed to accommodate a heavy cantilevered load, based on the expected weight of the detector and shielded collimator assembly. The detector support assembly is constructed such that when the detector is positioned inside the shielded collimator assembly, the center of the detector is at the axial midpoint of the fueled region of the pins mounted in the lattice plates. A sketch of the experimental apparatus is shown in Figure 2.

Fuel pin arrangements

The SPERT fuel pins used in the RCF core resemble commercial nuclear fuel rods with some notable differences in height and cladding material. Dimensions for the RCF fuel pins are provided in Table The fuel consists of UO_2 pellets, enriched to 4.81 wt. %

The fuel pellets are stacked in the pin and held in place with a spring in the upper plenum region. The stainless steel cladding consists of an upper end cap, tube, and lower end cap. The upper end cap contains a notched region to facilitate fuel handling and the lower end cap is equipped with a small dowel for positioning within the lower lattice plate. The pellet-clad gap and plenum region is filled with helium gas.

Fuel pins were arranged in the lattice plates to achieve the desired lattice configuration. In order to maximize the counts in the pulse-height spectra measured, the detector and collimator were positioned as close as possible to the fuel pin lattice without interfering with the range of motion of the lattice. The fuel pin arrangements consisted of a 3x3, 5x5, and 7x7 lattice. For each lattice arrangement, two sets of measurements were taken. One set of measurements was taken with the source pin in the middle of the lattice and the other set was taken with the source pin positioned in the far corner of the lattice.

Figure 3 shows a typical arrangement of the fuel pins, detector, and collimator with the source pin in the center and in the corner lattice positions.

Detector and Instrumentation

The RCF gamma-ray spectroscopy system consists of a NaI(Tl) detector with a 5.1 cm by 5.1 cm crystal (Canberra Model 802-2x2) connected to a photomultiplier tube and preamp (Canberra Model 2007P). The detector interfaces with a PC using a multichannel analyzer card (Canberra Model ASA-100). Data are collected, displayed and processed with spectroscopy software (Canberra GENIE-2000). The detector rests inside a lead brick shield with a collimator open to the fuel pin lattice. The collimator is 10.16 cm 5.08 cm high and 0.95 cm wide.

III. EXPERIMENTAL PROCEDURE

Setup

For all measurements performed, the same basic procedure was followed. While the RCF staff prepared the reactor for operation, the desired fuel pin arrangement was loaded into the experimental apparatus, less the source pin.

The detector and spectroscopy system were checked for proper operation and calibrated for that day's measurement. Channel calibration and detector efficiency curves were generated using a multi-gamma ray standard source. After being repositioned within the lead shield and collimator assembly, the detector was placed in position as close as possible to the lattice.

Four "regions of interest" (ROIs) were established within the pulse-height spectrum: 180 – 450 keV, 550 - 1000 keV, 1000 – 2000 keV, and 2000 – 3000 keV. The 450 – 550

keV portion of the spectrum was intentionally omitted to avoid the annihilation peak at 51 keV from pair-production reactions in the lead collimator.

For this series of measurements, the RCF core contained enough excess reactivity to achieve a constant period of approximately 26 s with control rods fully withdrawn. From previous measurements, it was expected that an adequate number of counts would be achieved using a source pin activated in the RCF core with an irradiation time of approximately 200 seconds corresponding to a power history of approximately 80 W·s. The activations were performed with all control rods fully withdrawn from the core. A sketch of the RCF core showing the location of the source pin and control rods is provided in Figure 4.

The target peak power level to achieve the desired irradiation time given a constant period of 26 s was calculated using the relationship

$$P(t) = P_{-\infty}e \tag{1}$$

where,

$P(t)$ = target peak power at time, t,

$P_{-\infty}$ = reactor power at beginning of history,

= reactor period.

The activation energy is the product of the power level and the time at that power level,

$$E = \int_{-\infty}^{t} dt' P_{-\infty} e^{\frac{t'}{\tau}} \tag{2}$$

Integrating Equation (2) is simple and results in

$$E = \tau \cdot P_{-\infty} e^{\frac{t'}{\tau}} \Big|_{-\infty}^{t} = \tau \cdot P_{-\infty} e^{\frac{t}{\tau}} \tag{3}$$

Substituting Equation (1) into Equation (3), the activation energy, E, given a constant period, τ, and a peak power, $P(t)$, is expressed as

$$E = \tau \cdot P(t) \tag{4}$$

Using Equation (4), it is now a straight-forward to calculate the desired peak power level given the expected reactor period and activation energy desired. With a 26 s period and 80 W·s activation, $P(t) = 3$. W. For reactor operator convenience, the target peak power level was set at 3 watts.

Once the desired peak power level was reached, the reactor was scrammed and a stopwatch started. Following several minutes to allow radiation levels to decrease, the center fuel pin was removed from the core of the RCF and transferred to the measurement apparatus. Table II provides the actual activation, time after scram that measurements commenced, and distance of the detector face from the source pin, for each measurement.

III.B Data Collection

Measurements commenced with a minimum of delay following transfer of the source pin to the measurement apparatus, usually within 5 – 10 minutes after the reactor was shutdown. The spectroscopy system was set up for 60 s counting intervals. Coincident with initiating a counting cycle, the time after scram was read from the stopwatch.

Initially, three measurements were taken at the reference position, defined as zero degrees lattice rotation. The lattice was then rotated to the 5 degree position for the fourth measurement. Measurement five was back at the reference position, followed by measurements six and seven at 10 and 15 degrees, respectively. This pattern was

followed to obtain data for nine more locations: 0, 20, 25, 0, 30, 35, 0, 40, and 45 degrees. Three final measurements were taken at the reference position.

The value of the integrated counts within a ROI, as reported by the spectroscopy system was recorded for each measurement along with the time after scram and angle of lattice rotation. Given the low activation level of the source pin, the instrument dead times were observed to be negligible. Table III shows the experimental data for the 7x7 pin lattice with corner pin activated.

III.C Data Reduction

The intensity of fission-product gamma rays constantly changes during the measurements due primarily to decay of short-lived isotopes. Therefore, in order to properly attribute changes in measured intensity to the channeling effect, a method of decay-correcting the recorded data was necessary. Previous measurements of the gamma-ray energy release as a function of time show that for the time period over which data was recorded for these measurements, the gamma-ray energy release rates as a function of time after fission are well-behaved. This suggests that the gamma-ray energy release rate as a function of time can be described by a single, continuous function.

Hence the need to record data at the reference position several times over the course of the measurement. By dividing the counts recorded at each ROI, $C(t)$, by the initial value, $C(0)$, a decay curve showing the fraction of the initial gamma-ray source strength versus time was generated. Figure 5 shows the normalized data points and the corresponding decay curves for each ROI, generated using a shifted-power fit of the form

$R(t) = A(t - B)^{-C}$ To decay-correct data, the measured value is divided by the corresponding value of the decay curve for that ROI at the time of the measurement

Decay curves describing the time-dependent photon emission at various energies are unique[1], suggesting that individual decay curves are necessary for each of the ROIs. Additionally, the sodium-iodide detector response will be affected by secondary radiations causing the pulse-height tallies in the lower energy ROIs to exhibit a more complex time-dependent behavior. For these reasons, decay curves for each ROI were generated.

IV. RESULTS

Results from the experimental measurements are shown in Figure 6 through Figure

Error bars corresponding to the 95% confidence intervals are provided for each point plotted. However, in most cases, the error bars are obscured by the symbols. The standard deviation was calculated by applying counting statistics to the collected data. An estimate of the standard deviation of a single measurement was made by assuming that the measured value is the mean, $\bar{x} = x$, and the count distribution follows a Poisson distribution. In making these two assumptions, the distribution is completely described and an estimate of the variance can be made where $\sigma^2 = \bar{x}$, or simply, $\sigma = \sqrt{x}$

The magnitude of the pulse heights is a function of the detector system efficiency for the ROI, the delayed gamma-ray spectrum for the ROI, and the penetrating power of the gamma rays in each ROI. Fission-product gamma rays are emitted with energy spanned by the first three ROIs at a higher probability than in the energy range spanned by the fourth ROI. Additionally, the efficiency of the detector system decreases as the incident gamma-ray energy increases. Considering these factors, it is not unexpected that the

highest energy ROI is well bellow the other three. For the purpose of this study, the decay-corrected counts are not normalized by the width of the ROI and it was not deemed necessary to correct for detector efficiency. The goal was to show the relative effect on gamma-ray dose from the channeling effect.

Caution must be exercised when comparing the absolute magnitudes of the plots shown in Figure 6 through Figure 11 The magnitudes are highly dependent on the distance from the source pin to the detector, the power history used to activate the source pin, and the time after reactor scram at which the counts were measured. These values vary from measurement to measurement, making comparisons based on magnitude difficult. However, the shapes of the curves and angles showing maximum channeling are considered most important for this study.

In all cases, the decay-corrected counts reach a maximum as the lattice is rotated through the first row of pins shielding it from the detector. In the case of the 3x3 lattice with center pin activated (Figure 6), there is just a single pin between the source and detector. As the angle of rotation reaches approximately 25 degrees, less and less of the pin is in line to the detector and the detector counts reach a maximum. Counts begin to decrease as the next pin is encountered and eventually approach the initial value at 45 degrees rotation, when the full diameter of the fuel pin is in-line between the source and detector.

For larger lattices, plots of decay-corrected counts versus degrees of lattice rotation are more complicated. Figure 7 shows the decay-corrected counts for the 3x3 lattice with the corner pin activated. In this configuration, the lattice must rotate approximately 15 degrees in order to reach the maximum. Figure 8 shows the decay-corrected counts for

the 5x5 lattice with the center pin activated. This plot is very similar in shape to Figure 6. This is expected considering that, relative to the detector, the number of pins rotating in and out of its path is identical to the 3x3 lattice with corner pin activated. Any difference between the two cases can be attributed to the contribution to the detector of multiple scattering of gamma rays off unirradiated fuel pins. In the 5x5 lattice with center pin activated, the source pin is surrounded on all sides by unirradiated pins whereas in the 3x3 lattice with corner pin activated, there are no pins behind or on one side of the source pin.

Figure 9 shows the decay-corrected counts for the 5x5 lattice with the corner pin activated. The maximum channeling for this lattice occurs between 5 and 10 degrees of lattice rotation. Additional peaks are also seen at approximately 20 and 30 degrees where the path to the detector intersects less fuel material. The conspicuous drop in the 180-450 keV ROI between 5 and 10 degrees, just as the other three ROIs are peaking, is probably due to sources of error beyond counting statistics, as will be presented in Section V

The decay-corrected counts for the 7x7 lattice, with center pin activated are shown in Figure 10. This lattice is less complex than the previous case in that a maximum of four fuel pins may fall between the source pin and detector. The maximum channeling occurs at approximately 10 degrees with a smaller peak at 25 degrees.

The most complicated lattice measured was the 7x7 lattice with corner pin activated. Figure shows the decay-corrected counts for this case. The maximum channeling occurs at approximately 5 degrees. Little additional structure is present in the plot and no significant channeling is measured beyond a slight drop at about 35 degrees. For this case, the measurement capability of the apparatus was probably the limiting factor. An

improved collimator and a method for a more precise positioning of the detector are necessary to achieve channeling data for more complicated lattice arrangements.

V. EXPERIMENTAL ERROR

Thus far, the only error attributed to the experimental measurements has been the counting error. In fact, however, the measurements are subject to many more sources of error based on the experimental setup used to collect the data.

In order to quantify some of the major sources of experimental error, a best estimate was made of the precision of some key parameters in the experimental setup: collimator slit width (Δw), detector offsets in the x and y axes (Δx and Δy), and lattice rotation ($\Delta\theta$). The top and bottom lattice plates were computer-machined to very tight tolerances in both position and hole diameter and are therefore not considered potential sources of error in the measurement. Figure 12 shows the potential sources of error investigated and Table IV shows the estimated precision of the measured parameters.

It was expected that the most complicated lattice would be the most sensitive to the sources of error in the experimental setup. MCNP calculations were performed using the 7x7 lattice, with the corner pin as the source, applying the estimated errors to the parameters in the computational model. The results were then compared to the base case. Table V shows the results of the error analysis. The estimated error is with respect to the base case. The 95% confidence intervals based on the uncertainties of the MCNP calculations are in the range of approximately 4% to 5%.

The experiment is most sensitive to the uncertainty in collimator slit width and lattice rotation, as determined from the MCNP analysis. The x and y axes offsets have less effect on the measurement, particularly after the first 10 degrees of lattice rotation.

During the course of any one particular set of measurements, any offset in the x or y axes and collimator slit are constant for each measurement. The error in rotating the lattice, however, will be random as the lattice is moved from position to position. Therefore, if all the parameters were at there presumed worst-case values, one estimate of the error expected in the measurement is 14% + 3% + 15% + 7% = 39%. For all the sources of error to be simultaneously at their maximum is unlikely. However, the potential for large errors in the measurements exist.

VI. CONCLUSIONS

The "channeling effect" was measured for six experimental lattice configurations; 3x3, 5x5, and 7x7 lattices, with both the corner position and center position containing the activated pin. The results of the measurements demonstrate that the gamma-ray radiation intensity on the outside of a lattice can vary widely, as a function of angle, within the plane of the lattice. The results presented here are intended to demonstrate the channeling effect for different lattice configurations and provide a basis for comparison to transport codes.

The decay-correction technique used to isolate the variation in measured counts due to lattice rotation versus decay of the fission-product source was satisfactory for these measurements. It was found that a separate decay-correction curve should be generated for every ROI in the pulse-height spectrum and for each set of measurements. Separate decay-correction curves improve the decay-corrected values of the measured data and improve the results of the measurements. Decay-correction curves can be generated for each set of measurements by recording the counts in each ROI at a set "reference"

position, e.g., zero degrees lattice rotation, several times over the course of the measurement.

An increase in precision for measuring the angle of rotation and the width of the collimator would have the greatest impact in increasing the confidence in the measurement. Although unlikely, there exists a potential for large cumulative errors to be introduced in the measurement if the apparatus positioning parameters were simultaneously at their worst-case values

REFERENCES

1. R.G. Jaeger, Editor, "Engineering Compendium on Radiation Shielding, Volume I," Springer – Verlag, New York (1968).

2. A. Bozkurt, N. Tsoulfanidis, "Modeling Gamma-Ray Dose Rate From A Spent Pressurized Water Reactor Fuel Assembly", Nuclear Technology, Vol. 119, (1997).

3. J. Y. Lee, H. D. Choi, "Pin Power Distribution Determined by Analyzing the Rotational Gamma Scanning Data of HANARO Fuel Bundle," Journal of the Korean Nuclear Society, Vol. 30, No. 5, (1998).

4. S. Jacobsson, C. Andersson, A. Hakansson, A. Backlin, "A Tomographic Method For Verification of the Integrity of Spent Nuclear Fuel Assemblies – I: Simulation Studies," Nuclear Technology, Vol. 135, (2001).

Table I. SPERT fuel pin dimensions (cm)

Overall height	113.35
Clad outside diameter	1.13
Clad thickness	0.05
Lower end cap length	2.54
Upper end cap length	4.45
Fuel height	91.44
Fuel pellet width	1.07

Table II. Core activation, time after SCRAM, and distance to detector for 3x3, 5x5 and 7x7 lattice LATDOSE calculations.

Lattice Configuration	Irradiation Time (s)	Peak Power Observed (W)	Reactor Period Measured (s)	Time after SCRAM (s)	Distance to Detector (cm)
3x3, center pin active	200	3.1	29	383	13.58
3x3, corner pin active	200	3.2	25	512	15.93
5x5, center pin active	200	3.4	26	471	15.30
5x5, corner pin active	200	3.1	26	425	20.31
7x7, center pin active	200	3.1	27	400	15.74
7x7, corner pin active	200	3.2	24	470	25.97

Table III. Experimental data of the measured counts as a function of lattice rotation for the 7x7 lattice with corner pin activated.

Count	Lattice Rotation (deg.)	Start Time After SCRAM (s)	Count Duration (s)	Effective Time After SCRAM (s)	180-450 keV (counts)	2σ	550-1000 keV (counts)	2σ
	0	440	60	470	19205		18734	
	0	536	60	566	16488		16304	
	0	619	60	649	15143		14613	
	5	720	60	750	26377		32453	
	0	815	60	845	12847		12091	
	10	923	60	953	13154		15377	
	15	1038	60	1068	12033		13796	
	0	1222	60	1252	10249		9479	
	20	1322	60	1352	11078		11916	
	25	1420	60	1450	10097		10910	
	0	1526	60	1556	9364		8471	
12	30	1830	60	1860	9275		9385	
13	35	1953	60	1983	8336		7893	
14	0	2054	60	2084	8089		7133	
15	40	2208	60	2238	7970		7348	
16	45	2314	60	2344	8095		7473	
17	0	2414	60	2444	7536		6631	163
18	0	2503	60	2533	7435		6610	163
19	0	2583	60	2613	7386		6505	161

Count	Lattice Rotation (deg.)	Start Time After SCRAM (s)	Count Duration (s)	Effective Time After SCRAM (s)	1000-2000 keV (counts)	2σ	2000-3000 keV (counts)	2σ
	0	440	60	470	12557		2157	
	0	536	60	566	10221		1640	
	0	619	60	649	8963		1403	
	5	720	60	750	21506		3497	
	0	815	60	845	7046		987	
	10	923	60	953	10814		1677	
	15	1038	60	1068	9241		1400	
	0	1222	60	1252	5091		600	
	20	1322	60	1352	7741		1068	
	25	1420	60	1450	6784		922	
	0	1526	60	1556	4247		470	
	30	1830	60	1860	5453		714	
	35	1953	60	1983	4112		481	
	0	2054	60	2084	3395		337	
	40	2208	60	2238	3220		339	
	45	2314	60	2344	3655		352	
	0	2414	60	2444	3074		266	
	0	2503	60	2533	2882		276	
	0	2583	60	2613	2953		261	

Table IV. Estimated precision for key parameters in the experimental setup.

Collimator Width	Δw	± 0.1 cm
X axis	Δx	± 0.2 cm
Y axis	Δy	± 0.2 cm
Lattice Rotation	$\Delta\theta$	± 1.0 degree

Table V. Estimated percent errors in measured counts as a function of lattice rotation for various sources of error in key parameters of the experimental setup.

	Lattice Rotation (degrees)									
Case	0	5	10	15	20	25	30	35	40	45
Collimator slit + 0.1 cm	14%	6%		9%	9%	14%				
y-axis offset = + 0.2 cm	3%	-3%		1%	1%	1%				
x-axis offset = + 0.2 cm	3%	-5%		2%	-3%	3%				
lattice rotation = + 1 deg	11%	-13%		-6%	3%	2%				
lattice rotation = - 1 deg	15%	-9%		4%	-4%	6%				
x-axis offset = - 0.2 cm	7%	-6%		-4%	0%	0%				

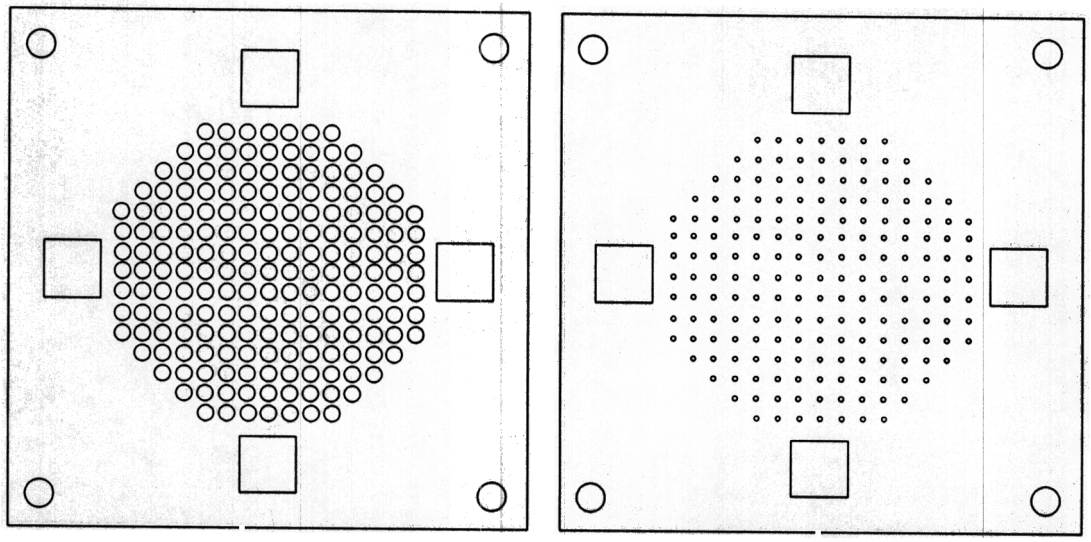

(a) (b)

Figure 1 Sketch showing top view of a typical (a) top lattice plate and (b) bottom lattice plate used in the experimental apparatus.

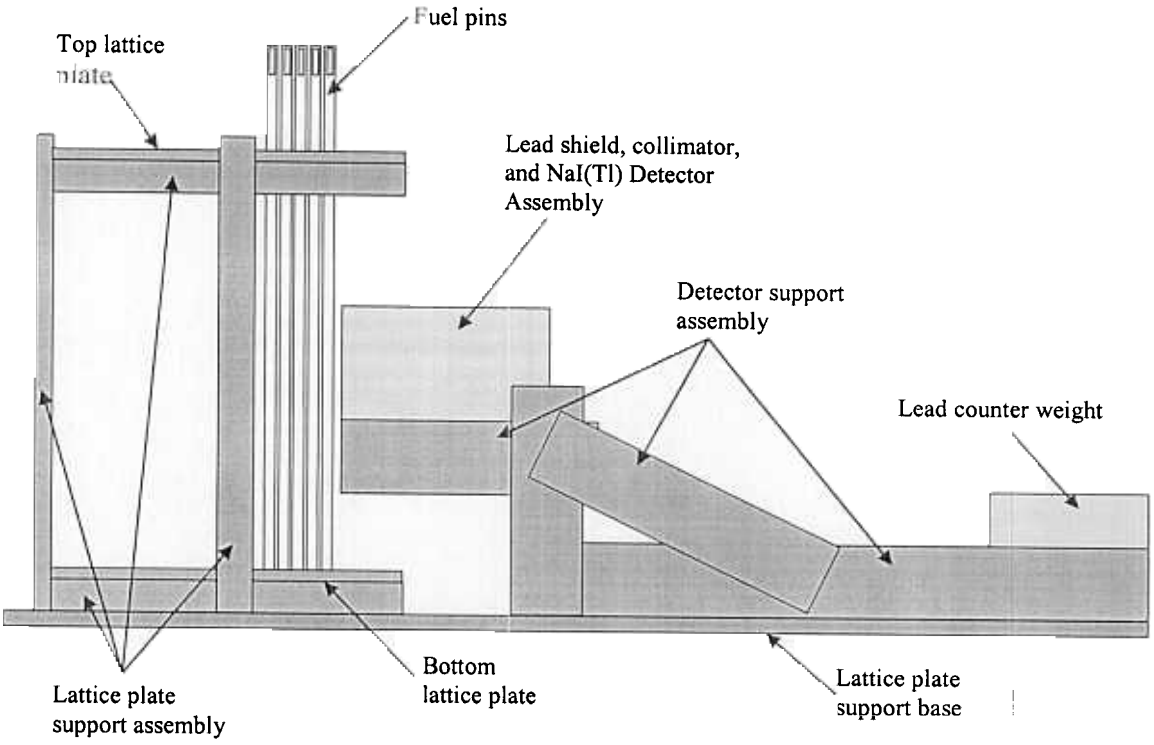

Figure 2. Sketch showing side-view of the experimental apparatus with fuel pins loaded and detector assembly positioned for measurements.

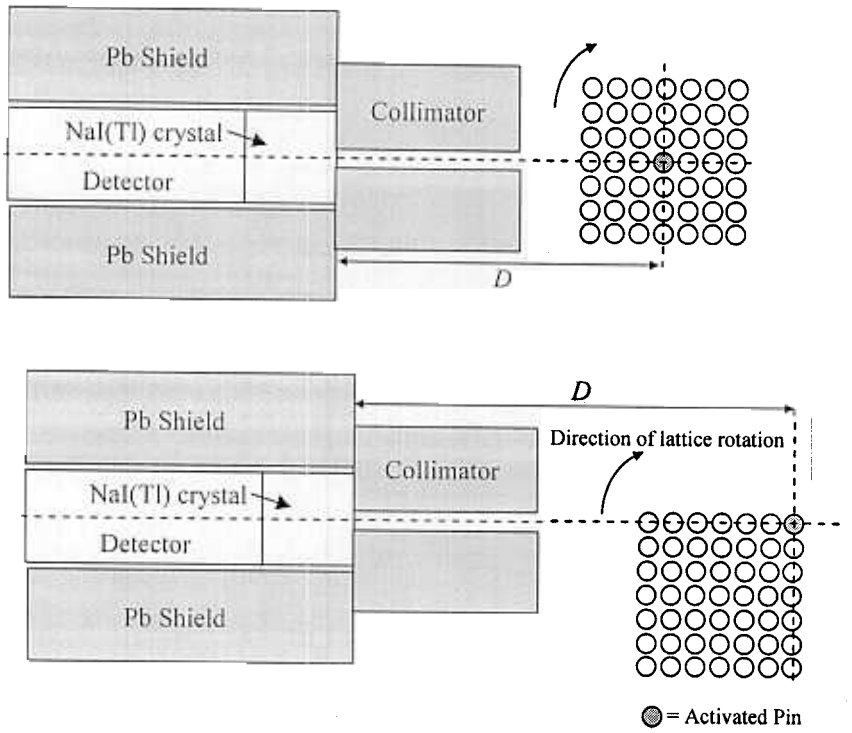

Figure 3. Top view of typical arrangement for detector, collimator, and fuel pin lattice with the activated pin in the center of the lattice (top) and corner of the lattice (bottom). In each case, the lattice is rotated about the activated fuel pin.

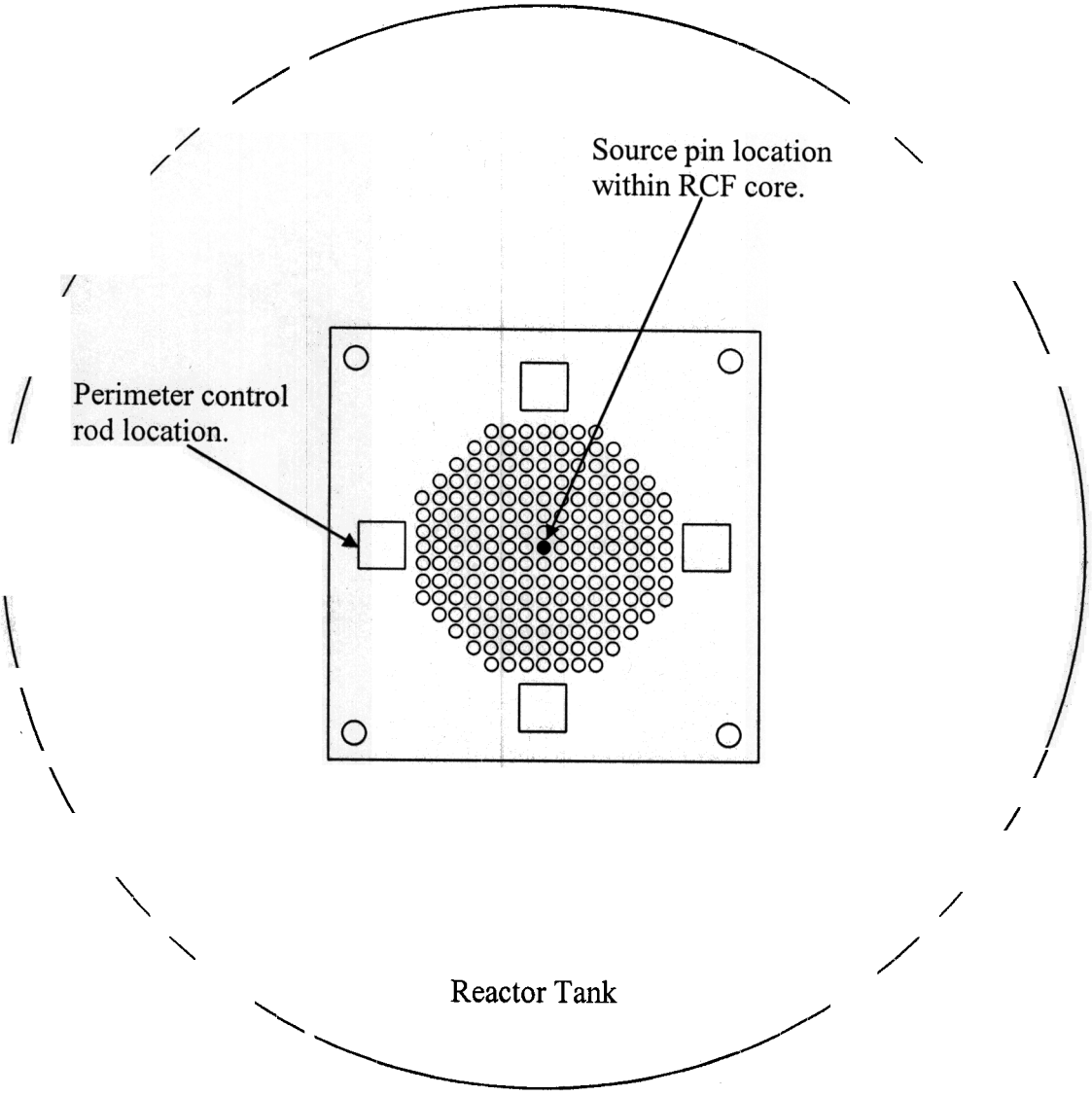

Figure 4. Sketch of the top view of the RCF reactor core showing the location of the source fuel pin and control rod arrangement.

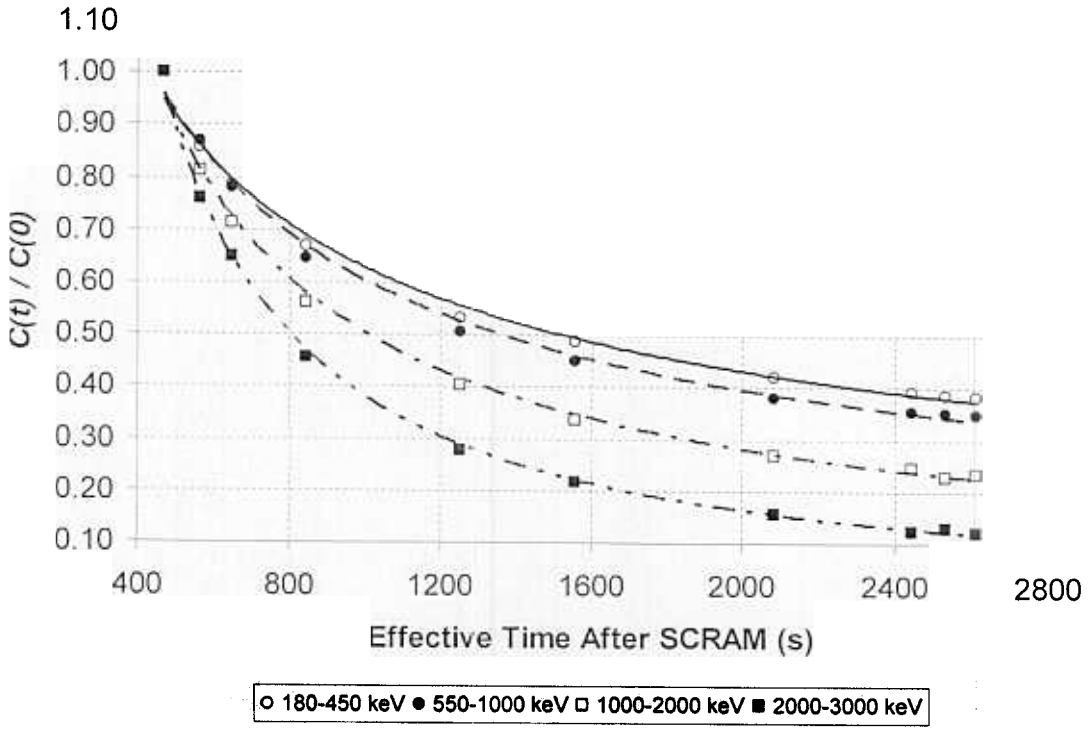

Figure 5. Fraction of initial counts versus time for each ROI at the reference position of the 7x7 lattice with fitted decay curves superimposed.

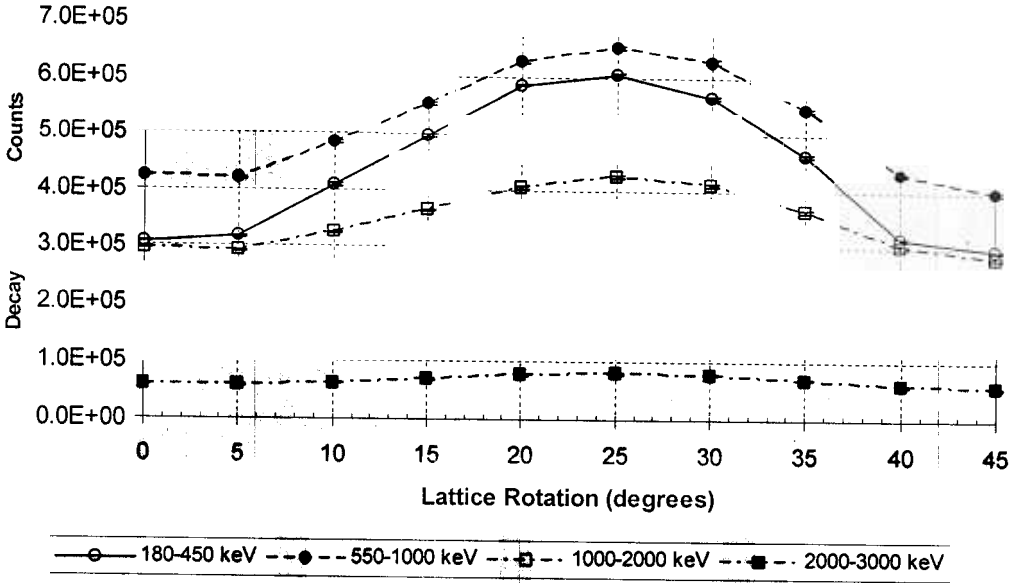

Figure 6. Decay corrected counts as a function of lattice rotation for each ROI using the 3x3 lattice with the center pin activated.

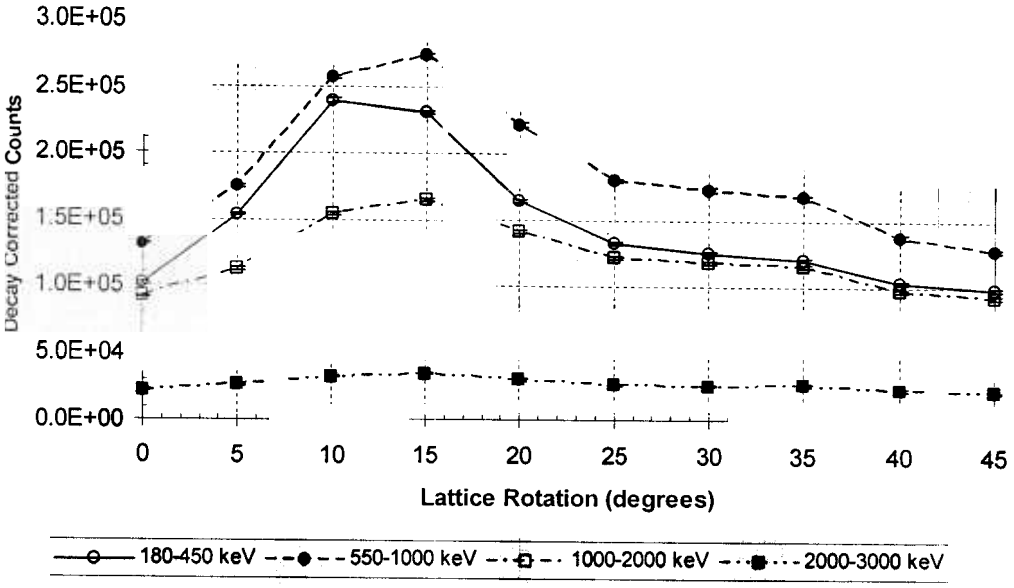

Figure 7. Decay corrected counts as a function of lattice rotation for each ROI using the 3x3 lattice with the corner pin activated.

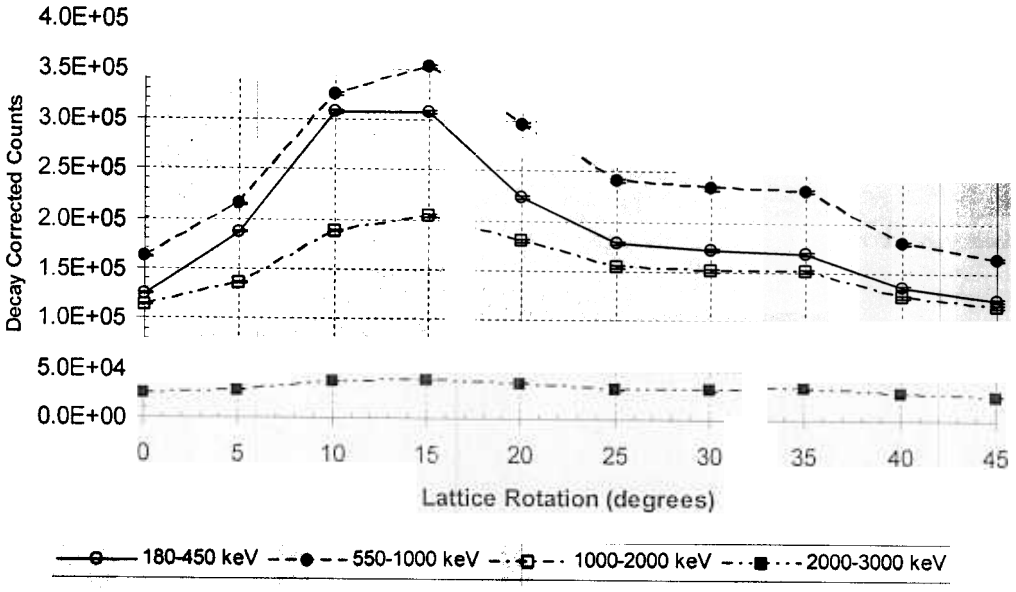

Figure 8. Decay corrected counts as a function of lattice rotation for each ROI using the 5x5 lattice with the center pin activated.

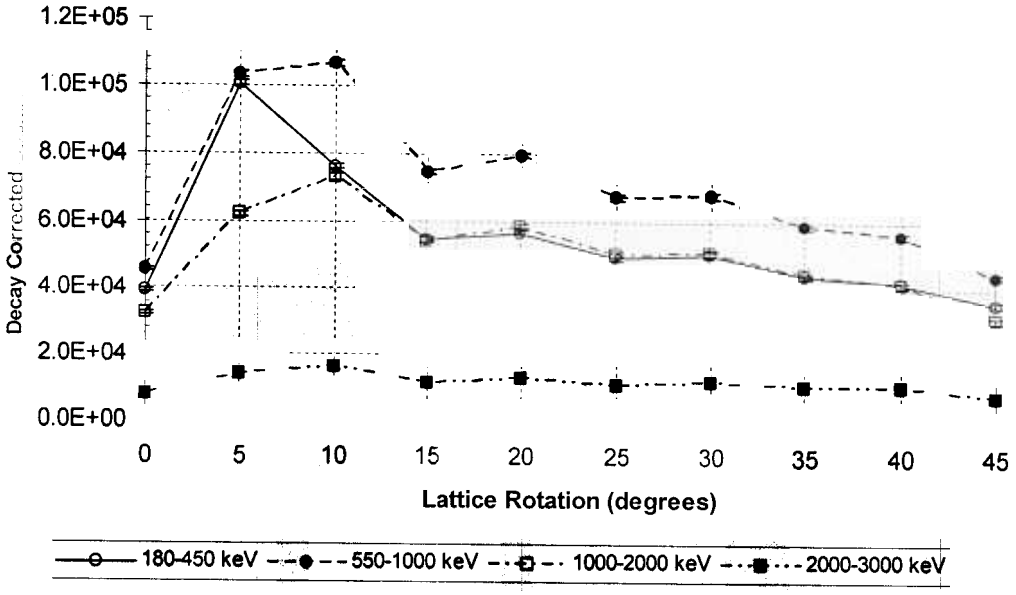

Figure 9. Decay corrected counts as a function of lattice rotation for each ROI using the 5x5 lattice with the corner pin activated.

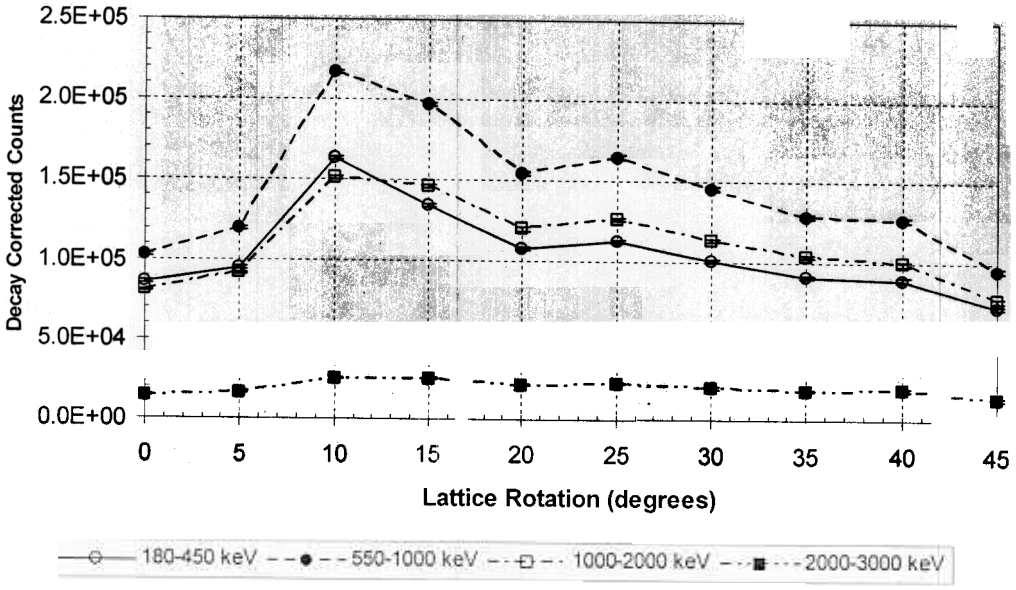

Figure 10. Decay corrected counts as a function of lattice rotation for each ROI using the 7x7 lattice with the center pin activated.

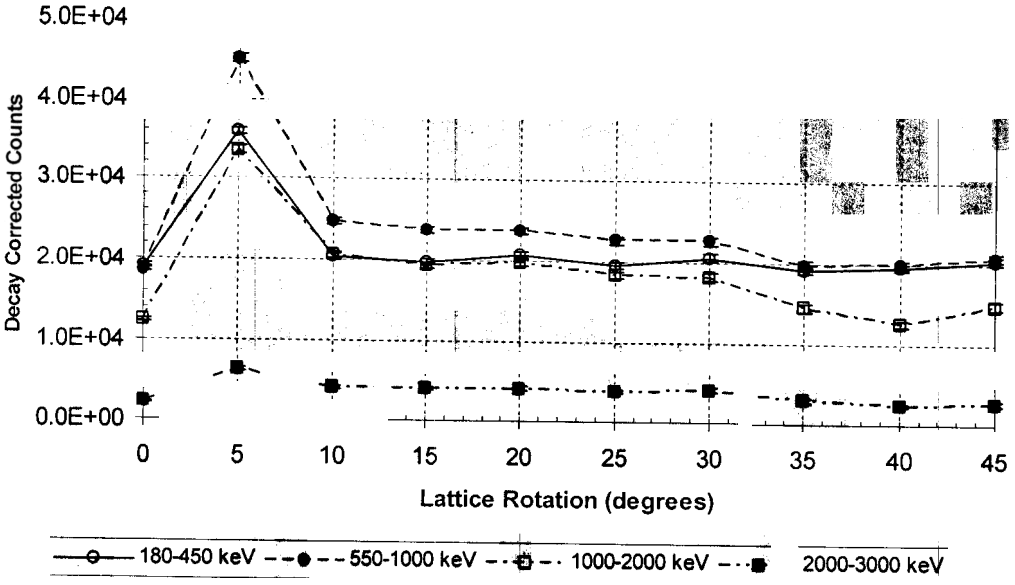

Figure 1 Decay corrected counts as a function of lattice rotation for each ROI using the 7x7 lattice with the corner pin activated.

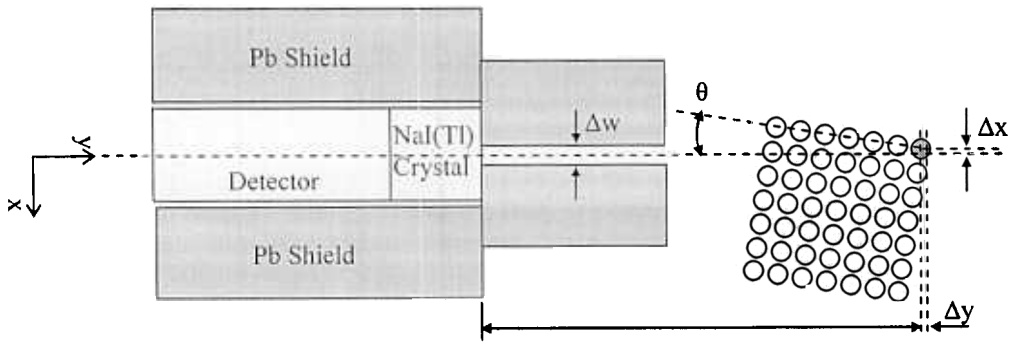

Figure 12. Top view schematic of 7x7 lattice measurements with corner pin activated showing potential sources of error in the experimental setup.